DC CONDUCTIVITY OF RF ABSORBING MATERIALS*

E. Chojnacki#, E. Smith, R. Ehrlich, M. Liepe and J. Sears
CLASSE, Cornell University, Ithaca, NY, U.S.A.

Abstract

Several of the typical RF absorbing materials utilized in particle accelerator environments have DC electrical conductivities that decrease significantly when cooled to cryogenic temperatures. If such RF absorbers are in close proximity to a beamline, they are prone to collecting static charge and may deflect the particle beam. The DC electrical conductivities of two types of ferrite and a ceramic are measured at various temperatures, showing that the electrical conductivities indeed decrease, often to unacceptably low levels in regard to static charge accumulation.

INTRODUCTION

RF absorbing materials are frequently utilized in particle accelerator environments. There are stringent requirements placed on some of these absorbers in regard to vacuum compatibility, radiation compatibility, and particulate generation, especially for absorbers in close proximity to the beamline, such as in some higher order mode (HOM) load designs. For RF absorbers located directly on the beamline, their DC conductivity must also be large enough to drain away static charge that may be deposited onto them by stray particles, otherwise, such static charge could deflect the particle beam. The beamline HOM load development efforts at Cornell have utilized the few materials that have been found to satisfy all of these requirements at room temperature [1-3].

A recent challenge has been for such beamline HOM loads to have similar performance at cryogenic temperatures. For the cryogenic application, the RF absorption properties at 77K have been tested and found to be acceptable [3], however, satisfying the DC conductivity to drain static charge can be challenging. The phenomenon familiar to materials scientists is that the activation energy can increase substantially with decreasing temperature, thus making band-gap type materials have DC conductivities that drop many orders of magnitude between 293K and 77K [4,5]. Thus, many materials are effectively insulators at 77K and will hold static charge for time scales easily much greater than days. In the following, tests and results for a few specific RF absorbing materials will be described.

RF ABSORBING MATERIALS

Typically, any given material has good RF absorption only in a band of frequencies. A collection of several materials can be implemented in an RF load to accomplish broadband absorption. To this end, Cornell has recently used the ferrites TT1-111R and Co2Z from Trans Tech [6] and the AlN-based composite Ceralloy® 137ZR10 from Ceradyne [7] in a prototype cryogenic beamline load [3]. This demanding application having 80K operation places obvious thermal expansion challenges on the materials. For this reason, the heat sink substrate to which the RF absorbers are bonded must be selected carefully.

The DC conductivities of these three types of RF absorbers were recently measured at 77K. The results presented below show that the materials do not obey a simple band-gap model where the DC electrical conductivity would have the form

$$\sigma \sim e^{-\theta/2kT} \quad , \tag{1}$$

where θ is the activation energy. However, the materials do show a similar dramatic decrease in electrical conductivity with decreasing temperature. The deviation of the materials from eq (1) has been reported to vary with oxidation state and has been attributed a distribution of energy levels within the forbidden gap [4].

Given that an RF absorbing material may have a low DC conductivity, a criteria is needed to decide whether it could be used in a specific application. One measure is the time constant required for static charge to drain through the bulk. Assuming the case with the longest conduction path where all of the charge is deposited on the surface of an absorber, the simple *RC* time constant for decay is

$$RC = \frac{\rho d}{A} \cdot \frac{\varepsilon A}{d} = \rho\varepsilon \ \text{[sec]} \quad , \tag{2}$$

where ρ is the material resistivity [Ω·m], ε is the dielectric constant [F/m], A is the area onto which charge is deposited, and d is the thickness of absorber material to the metallic substrate at ground potential.

MEASUREMENT TECHNIQUE

Measurements of DC conductivity of the RF absorbers were performed in two ways for this study. In the first technique, copper electrodes were simply clamped across opposite faces of a 3 mm thick absorber tile, as shown in Fig. 1. A voltage was applied to the electrodes and the current measured with an ammeter. The maximum resolvable resistance of the set up was about 1 TΩ. A few measurements were performed at elevated temperatures up to 398K (125C) to obtain additional data points for curve fitting, but most measurements were performed at room temperature 293K and below. The convenient bath temperatures utilized were water ice at 273K, dry ice at 195K, and liquid nitrogen at 77K. An example of the liquid nitrogen measurement is shown in Fig. 2.

A second DC conductivity measurement technique was used to minimize the effect of contact impedance between the copper electrodes and the RF absorber. To accomplish

* Work supported by NSF, New York State, and Cornell University
# epc1@cornell.edu

this, one face of the absorber tile was sputter coated with copper, the center portion of the copper sanded off, and copper electrodes soldered to the end stripes of copper, as shown in Fig. 3. The measurements with soldered electrodes gave similar results for conductivity as the clamped electrode technique, thus eliminating contact impedance as a large contributor to measured resistances, both in the kΩ range and in the TΩ range.

To convert a measured resistance to a material bulk conductivity, or resistivity, the electrode configurations were modeled in ANSYS. In the models, the bulk resistivity was set to 1 Ω·m, and boundary conditions of ±1 Ampere were placed on the electrode surfaces, as shown in Fig. 4 for the setup of Fig. 3 with soldered electrodes. ANSYS returns the voltage difference between the electrodes, from which the resistance between electrodes is obtained by

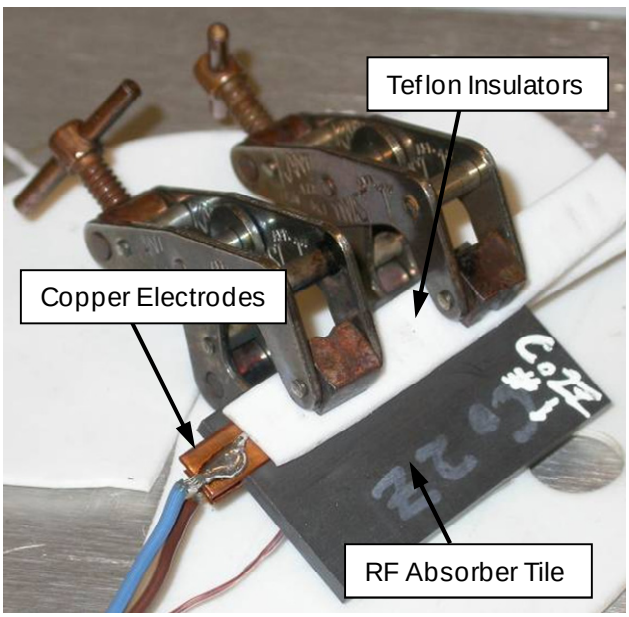

Figure 1: The first measurement configuration of DC conductivity by clamping copper electrodes across opposite faces of a 3 mm thick RF absorber tile.

Figure 2: Measurement of DC conductivity at 77K in liquid nitrogen.

$$R_{sim}(\rho = 1) = V_{sim} / I_{sim} \quad , \tag{3}$$

where I_{sim} = 1 A. The bulk resistivity of an RF absorber having the modeled electrode configuration is then obtained from the measured resistance by

$$\rho_{meas} = R_{meas} / R_{sim}(\rho = 1) \quad . \tag{4}$$

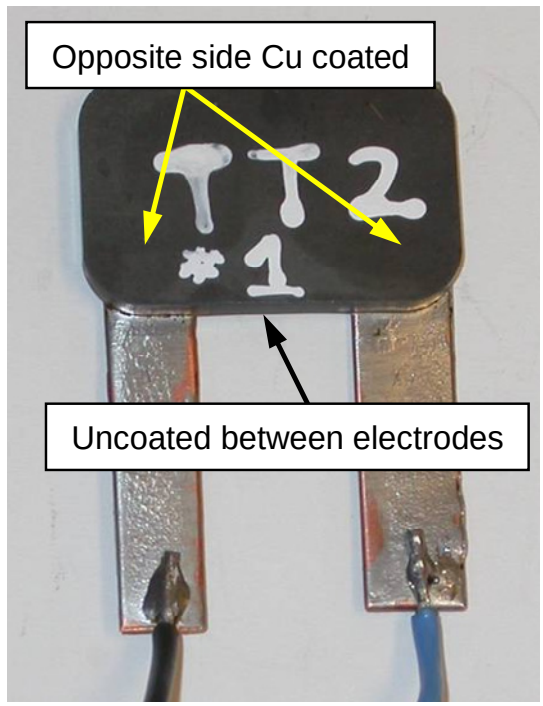

Figure 3: The second measurement configuration of DC conductivity by soldering copper electrodes to a copper sputter coated face of a 3 mm thick RF absorber tile.

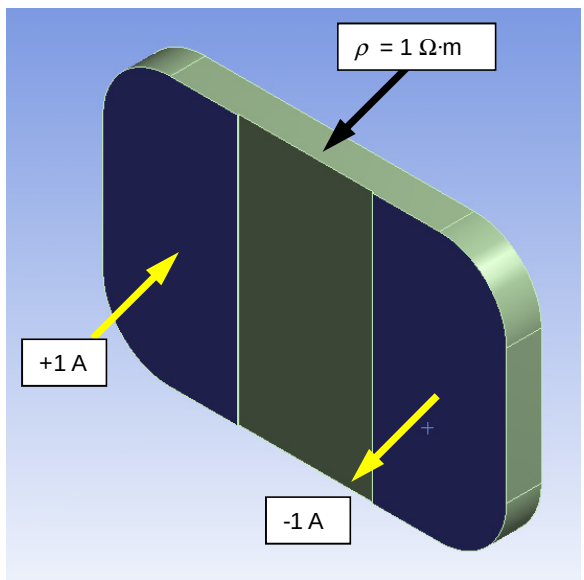

Figure 4: ANSYS model of the setup of Fig. 3 to obtain the voltage difference between electrodes for a baseline bulk resistivity ρ = 1 Ω·m.

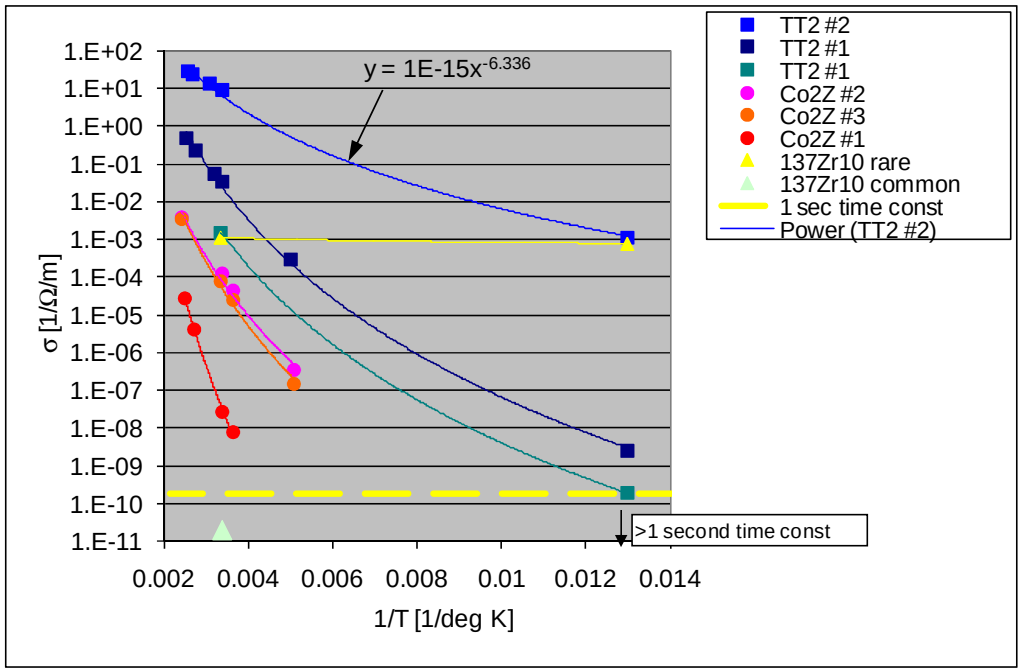

Figure 5: Conductivity of RF absorber materials and the threshold for 1 second time constant.

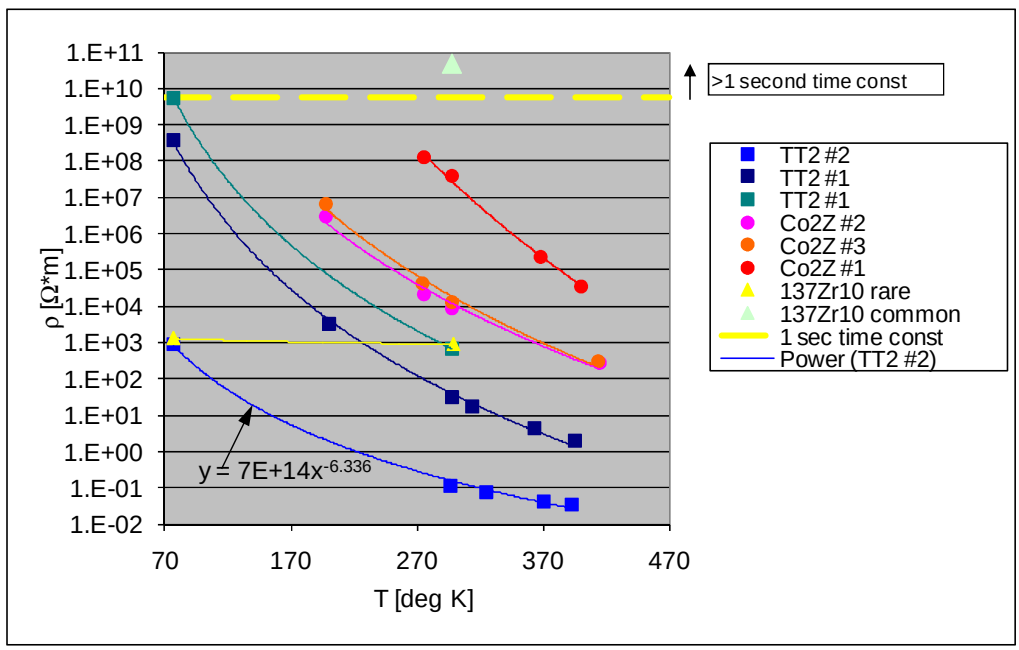

Figure 6: Resistivity of RF absorber materials and the threshold for 1 second time constant.

MEASUREMENT RESULTS

The sequence of electrical conductivity measurements consisted of first determining whether the conductivity follows the bandgap model of Eq. 1. Then, numerous samples were measured to determine the variability of conductivity among samples of the same type of absorber. Lastly, the effect of firing the tiles in air at 900°C was determined by measuring the conductivity before and after air firing.

Curve Fit

The first set of conductivity measurements of the three types of RF absorber are shown in terms of conductivity in Fig. 5 and in terms of resistivity in Fig. 6. For these measurements, additional data points were taken above room temperature to obtain a greater range for the curve fits. If a simple bandgap model were to describe the material conductivity, as in Eq. 1, the plots in Fig. 5 should linear. However, as seen in the figure, the best fit is a power law. The deviation of the materials from Eq. 1

has been reported to vary with oxidation state and has been attributed a distribution of energy levels within the forbidden gap [4].

Note in Figs. 5 and 6 that Ceralloy® 137ZR10 has just a few data points. The reason is that the great majority of these samples had very high resistivity at room temperature, and increased to above measurement range with cooling only to water ice at 273K. This is indicated by the data point labeled "Ceralloy common" in the legend. There was a single sample of 137ZR10 that had low resistivity at room temperature with negligible increase when cooled to 77K. This is indicated by the data point labeled "Ceralloy rare" in the legend.

Variability of Samples

Shown in Fig. 7 are resistivity measurements of numerous samples of TT2 and Co2Z ferrite at room temperature 293K and a cold temperature of either 77K or 195K. The resistivity of Co2Z increased to above measurement range at 77K, so the cold measurement for Co2Z was performed with dry ice at 195K. To help distinguish the TT2 from Co2Z in Fig. 7, the data points per sample are connected by straight lines, though power-law curve fits are shown for representative TT2 and Co2Z. It is seen in Fig. 7 that TT2 has about two orders of magnitude lower resistivity than Co2Z. The typical charge decay time constant for TT2 at 77K is less than 0.1 second, but the time constant for Co2Z is expected to exceed 30 seconds.

Firing in Air at 900°C

The ferrite tile processing employed at Cornell for HOM loads included firing the tiles as received from the manufacturer in air at 900°C for two hours. Ostensibly, this was performed to obtain fewer oxidation states and establish consistent material properties. To test whether the air firing effected DC resistivity, measurements were performed on ferrites as received from the manufacturer both before and after firing in air at 900°C. The results are shown in Fig. 8 for TT2 and in Fig. 9 for Co2Z. It is seen in both of these figures that firing in air increases the electrical resistivity by about a factor of 10 for both TT2 and Co2Z. The air firing increased the resistivity of TT2 ferrite to above measurement range at 77K, thus the 195K measurement point in Fig. 8 after firing. The air firing increased the resistivity of Co2Z ferrite to above measurement range even at 195K, thus only a 293K measurement point in Fig. 9 after firing.

ELECTRON BEAM TESTS

To obtain a visual indication of RF absorber electrical conductivity, samples were placed in an electron beam welder where a copious amount of charge is generated. The absorber tiles were mounted on edge on a support plate, the assembly cooled to about 90K, and the e-beam passed parallel to the face of the tile. The spot where the e-beam strikes the support fixture was observed, as shown in Fig. 10. As the beam was scanned parallel to the tile,

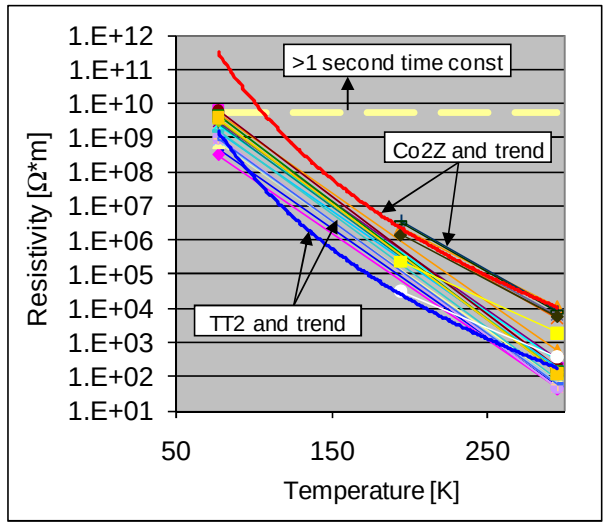

Figure 7: Numerous resistivity measurements of TT2 and Co2Z.

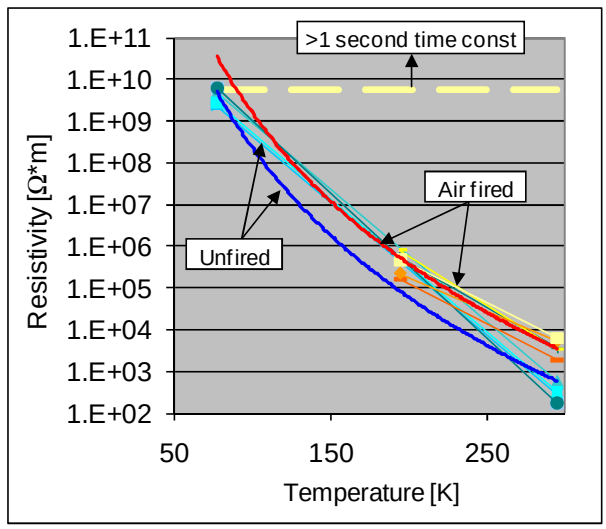

Figure 8: Resistivity of TT2 before and after firing in air at 900°C.

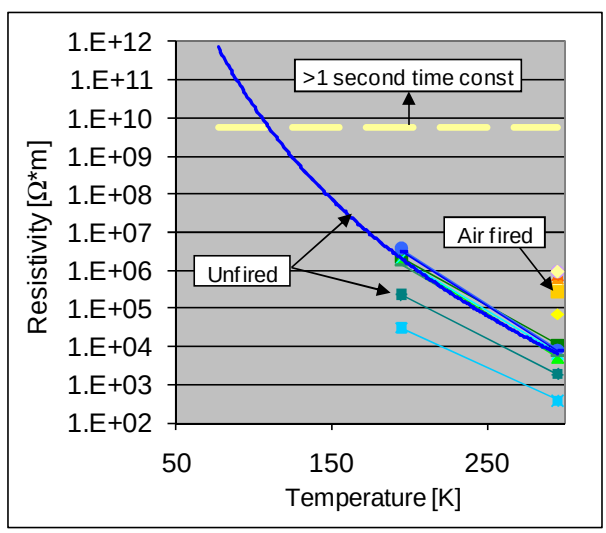

Figure 9: Resistivity of Co2Z before and after firing in air at 900°C.

the deflection of the electron beam was compared to a straight line that is obtained when a simple metal conductor is placed in the tile location. The Ceralloy® 137ZR10 tiles charged and deflected the e-beam even at 293K. Further, regions of the 137ZR10 tiles glowed, as seen in Fig. 10, where the glow correlated to regions with better electrical conductivity. The TT2 and Co2Z ferrites did not deflect the e-beam at 293K. The Co2Z at 90K deflected the e-beam to a similar degree as 137ZR10, although without glowing. The TT2 at 90K deflected the e-beam about half as much as did the other absorbers. These qualitative static charge tests are consistent with the electrical conductivity measurements described above.

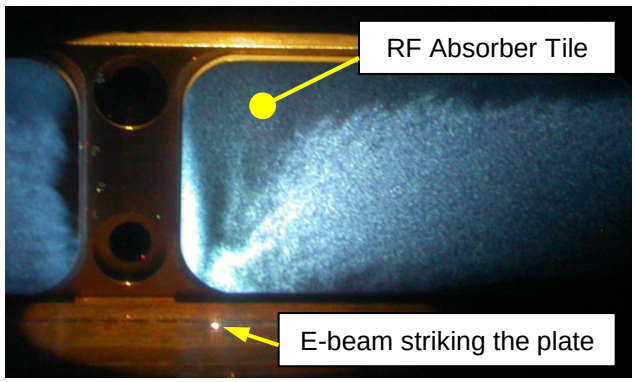

Figure 10: Electron beam welder static charge test of a Ceralloy® 137ZR10 RF absorber tile.

SUMMARY

The DC electrical conductivities of several typical RF absorbing materials utilized in particle accelerator environments were measured at various temperatures. The conductivity of all of the materials was observed to decrease significantly when cooled to cryogenic temperatures. The ferrite TT2-111R maintains a modest electrical conductivity at 77K of $\sigma \sim 5\times10^{-10}$ $(\Omega\cdot\mathrm{m})^{1}$, or resistivity $\rho \sim 2\times10^{9}$ $(\Omega\cdot\mathrm{m})$. This corresponds to a static charge decay time constant of about 0.1 second. Whether such an electrical conductivity is acceptable depends on the specific application's beam energy, particle species, and expected amount of charge deposition on the RF absorber.

REFERENCES

[1] D. Moffat, *et al.*, "Design and Fabrication of a Ferrite-lined HOM Load for CESR-B", PAC'93 Washington, DC, p. 977, http://accelconf.web.cern.ch/AccelConf/p93/PDF/PAC1993_0977.PDF

[2] E. Chojnacki and W. J. Alton, "Beamline RF Load Development at Cornell", PAC'99 Washington, DC, p. 845, http://accelconf.web.cern.ch/AccelConf/p99/PAPERS/MOP77.PDF

[3] V. Shemelin, M. Liepe, and H. Padamsee, "Characterization of Ferrites at Low Temperature and High Frequency" Nucl Instr and Meth in Phys Res A Vol. 557, p.268 (2006).

[4] C.F. Jefferson and C.K. Baker, "Mechanism of Electrical Conductivity in Nickel-Iron Ferrite", IEEE Trans Mag, MAG-4, No. 3, p. 460 (1968).

[5] J.R. Drabble and T.D. Whyte, "The Direct Current Measurement of Very High Resistance at Low Temperatures", J Phy E: Scientific Instr, Vol 3, p.517 (1970).

[6] Trans-Tech, Inc., Adamstown, MD, http://www.trans-techinc.com/

[7] Ceradyne Inc., Costa Mesa, CA, http://www.ceradyne.com/